

# Electromagnetic wave transmission through a small hole in a perfect electric conductor of finite thickness

A. Yu. Nikitin<sup>1,2,\*</sup>, D. Zueco<sup>1†</sup>, F. J. García-Vidal<sup>3</sup>, and L. Martín-Moreno<sup>1‡</sup>

<sup>1</sup> *Instituto de Ciencia de Materiales de Aragón and Departamento de Física de la Materia Condensada, CSIC-Universidad de Zaragoza, E-50009, Zaragoza, Spain*

<sup>2</sup> *Theoretical Physics Department, A.Ya. Usikov Institute for Radiophysics and Electronics, Ukrainian Academy of Sciences, 12 Acad. Proskura Str., 61085 Kharkov, Ukraine*

<sup>3</sup> *Departamento de Física Teórica de la Materia Condensada, Universidad Autónoma de Madrid, E-28049 Madrid, Spain*

The non-resonant electromagnetic transmission of a normal-incident plane wave through a single hole in a perfect conductor metal slab of finite width is studied. The cases of rectangular and circular holes are treated in detail. For holes in the extreme subwavelength regime, in a film of finite thickness, the transmittance is shown to have the Rayleigh dependency upon the wavelength and, in addition, is mainly suppressed due to attenuation of the fundamental waveguide mode. In the limit of an infinitesimally thin screen Bethe's result is recovered for the circular hole. The numerical computations are fitted, providing expressions for the transmission in a wide region of parameters. We reformulate our results in terms of multipole expansion, interpreting the waveguide modes inside the hole as induced multipole moments. This result provides the link between the modal expansion method and the one based on a multipole expansion.

PACS numbers: 42.25.Bs, 41.20.Jb, 42.79.Ag, 78.66.Bz

## I. INTRODUCTION

Electromagnetic (EM) wave transmission through apertures in perfect metal screens has been the subject of multiple studies. For a long time, up to the middle of XX century, theoretical treatments of diffraction by either opaque or metal bodies based on the Kirchhoff approach. This method consists in setting the fields on the body equal to their incident values. Bethe was the first to consider the diffraction by a small circular aperture of radius  $a$  in an infinitesimally thin perfectly conducting screen, providing rigorous analysis of the Maxwell's equations with the exact boundary conditions in 1944.<sup>1</sup> He found analytically the pre-factor appearing in the well-known Rayleigh scattering dependency  $\sim (a/\lambda)^4$  for the scattering cross-section of small objects in the long-wavelength limit ( $a \ll \lambda$ ). Later on, Bowkamp improved Bethe's result, providing additional terms in a series expansion of the transmission over  $a/\lambda$ . Since then, this kind of diffraction problem has become a classical chapter in many monographs on electromagnetism, e.g., Refs. 2,3.

The interest in EM transmission through apertures has been renewed thanks to the discovery in 1998 of the enhanced optical transmission through an array of small holes.<sup>4</sup> A great deal of research has been devoted to the transmission through periodical arrays of the holes. Nevertheless, the analysis of the diffraction

by a single hole in a film of finite thickness is still incomplete, as results found in the literature are only for fixed geometrical parameters. For example, Refs. 5,6 provide computed transmission spectra through a circular hole in a film of a finite thickness in a perfect electric conductor (PEC) slab. The case of a single circular hole in a real metal has been considered in Refs. 7,8,9. However, it is problematic to extrapolate these results to other parameters and other hole shapes. An attempt to represent the solution in an analytical form was undertaken in Ref. 10. These authors derived the normalized cross section for a circular aperture (of radius up to half of the wavelength in PEC) assuming that the magnetic current is uniform within the aperture. Nevertheless, this model shows poor quantitative agreement with both the Bethe-Bouwkamp results and the strict numerical calculations of Roberts.<sup>5</sup> Moreover, it is limited to a screen with zero thickness.

In this paper we study the optical transmission through single holes in PEC. We present new analytical results, valid for a wide range of geometrical parameters, and provide a link between the modal expansion method and the one based on multipoles. The paper is organized as follows: In Section II we describe the modal expansion technique used for studying the transmission through the hole in a perfect electric conductor film of arbitrary thickness. In Section III we provide analytical expressions for the transmission through holes of both rectangular and circular shapes in extreme subwavelength limit. We test our approach by applying it to the most unfavorable conditions for the method used (when the film thickness is zero), and obtain an excellent agreement with known results. In

---

<sup>†</sup>Present address: Institut für Physik, Universität Augsburg, Universitätsstraße 1, D-86135 Augsburg, Germany

Section IV the square hole of moderate size is treated, when the wavelength is still larger than the hole cutoff (therefore, the resonances found close to cutoff<sup>11,12,13</sup> will not be discussed there, as have already been addressed before<sup>14,15</sup>). Finally, in Section V, we make the link between the induced multipoles and the waveguide modes inside the hole. We discuss the importance of the fundamental waveguide mode both for the formation of the induced dipole moments on both faces of the hole and for the coupling between these moments. In Appendix we explain the simplifications of Green's tensor for the small hole limit.

## II. THEORETICAL BACKGROUND

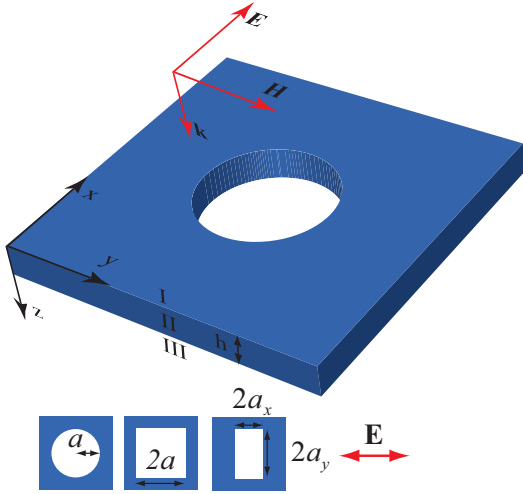


FIG. 1: (Color online) Geometry of the problem.

In this section we briefly outline the modal expansion formalism for the EM field.<sup>14,16</sup> Consider an EM wave incident onto a PEC film of finite thickness  $h$  containing a hole, see Fig.1. We first assume that both the bounding media and the medium inside the aperture is vacuum, but later on we generalize the results to arbitrary values of the optical indices of the semi-infinite media.

For the representation of the EM field in-plane components we use Dirac's notations as follows. The projection of a given Dirac's vector onto the position vector  $|\mathbf{r}_t\rangle$ , with  $\mathbf{r}_t = (x, y)$ , simply yields the value of Dirac's vector in the position  $\mathbf{r}_t$  coordinate dependent field in the coordinate space, for example:

$$\langle \mathbf{r}_t | \mathbf{E} \rangle = \mathbf{E}_t(x, y). \quad (1)$$

The projection of a vector onto another one is given by the scalar product

$$\langle \alpha | \kappa \rangle = \int d\mathbf{r}_t \langle \alpha | \mathbf{r}_t \rangle \langle \mathbf{r}_t | \kappa \rangle^*, \quad (2)$$

where “\*” means complex conjugation.

Let us write in Dirac's notations the tangential components of the fields in the lower and upper half-spaces, expanding them over the continuum of plane waves (see the geometry in Fig. 1):

$$\begin{aligned} |\mathbf{E}_I(z)\rangle &= e^{ik_z z} |\kappa_i\rangle + \sum_{\kappa} r_{\kappa} e^{-ik_z z} |\kappa\rangle, \\ |\mathbf{E}_{III}(z)\rangle &= \sum_{\kappa} t_{\kappa} e^{ik_z(z-h)} |\kappa\rangle. \end{aligned} \quad (3)$$

Here  $\kappa = (\mathbf{k}, \sigma)$  represents both the in-plane wavevector component  $\mathbf{k} = (k_x, k_y)$  and the polarization,  $\sigma = p$  or  $\sigma = s$ . The coordinate representation of the modes in the vacuum half-spaces reads

$$\langle \mathbf{r}_t | \mathbf{k}, s \rangle = \begin{pmatrix} -k_y \\ k_x \end{pmatrix} \frac{e^{i\mathbf{k}\mathbf{r}_t}}{k}, \quad \langle \mathbf{r}_t | \mathbf{k}, p \rangle = \begin{pmatrix} k_x \\ k_y \end{pmatrix} \frac{e^{i\mathbf{k}\mathbf{r}_t}}{k}. \quad (4)$$

The plane wave propagation constant is  $k_z = \sqrt{g^2 - k^2}$  with  $g = 2\pi/\lambda$ . The summation operator in Eq. (3) includes both the integration over the  $k$  continuum spectrum and the summation over the polarizations:  $\sum_{\kappa} = (1/2\pi)^2 \sum_{\sigma} \int d\mathbf{k}$ . Inside the hole, we expand the tangential components of the field over the modes  $|\alpha\rangle$  of the infinite waveguide

$$|\mathbf{E}(z)\rangle = \sum_{\alpha} (A_{\alpha} e^{iq_{z\alpha} z} + B_{\alpha} e^{-iq_{z\alpha} z}) |\alpha\rangle, \quad (5)$$

where  $A_{\alpha}$  and  $B_{\alpha}$  are the amplitudes of the waveguide modes propagating (or decaying) forwardly and backwardly with respect to  $z$ -axis direction;  $q_{z\alpha}$  represents the propagation constant of a waveguide mode with the label  $\alpha$ . This label contains both the polarization of the waveguide mode and a “spatial” index related to the number of nodes of the field inside the hole.

By matching the EM fields at the interfaces, and using the orthogonality of the modes, we arrive at a set of linear equations for the expansion coefficients

$$\begin{aligned} (G_{\alpha\alpha} - \Sigma_{\alpha}) E_{\alpha} + \sum_{\alpha \neq \beta} G_{\alpha\beta} E_{\beta} - G_{\alpha}^V E'_{\alpha} &= I_{\alpha}, \\ (G_{\gamma\gamma} - \Sigma_{\gamma}) E'_{\gamma} + \sum_{\nu \neq \gamma} G_{\gamma\nu} E'_{\nu} - G_{\gamma}^V E_{\gamma} &= 0. \end{aligned} \quad (6)$$

The coefficients  $E_{\alpha}$  and  $E'_{\alpha}$  are

$$\begin{aligned} E_{\alpha} &= A_{\alpha} + B_{\alpha}, \\ E'_{\alpha} &= -(A_{\alpha} e^{iq_{z\alpha} h} + B_{\alpha} e^{-iq_{z\alpha} h}), \end{aligned} \quad (7)$$

so that the system of Eqs. (6) connects the electric field modal amplitudes on the incoming interface,  $z = 0$ , and on the outgoing one,  $z = h$ . The term  $G_{\alpha}^V$  describes the coupling between the input and output sides of the holes, and  $\Sigma_{\alpha}$  arises from the reflection of the waveguide mode at the openings:

$$G_{\alpha}^V = \frac{2iY_{\alpha} e^{iq_{z\alpha} h}}{e^{2iq_{z\alpha} h} - 1}, \quad \Sigma_{\alpha} = iY_{\alpha} \frac{e^{2iq_{z\alpha} h} + 1}{e^{2iq_{z\alpha} h} - 1}, \quad (8)$$

where  $Y_\alpha = q_{z\alpha}/g$  is the admittance for the TE waveguide mode, and  $Y_\alpha = g/q_{z\alpha}$  is that for the TM one. The coupling matrix elements of the system of Eqs. (6) are related to the in-plane components of the EM Green function dyadic  $\hat{G}$ . The latter is associated to a homogeneous medium in three dimensions and is represented in the waveguide mode space:

$$G_{\alpha\beta} = \langle \alpha | \hat{G} | \beta \rangle = i \sum_{\kappa} Y_{\kappa} \langle \alpha | \kappa \rangle \langle \kappa | \beta \rangle. \quad (9)$$

Here  $Y_{\kappa}$  is the admittance of the mode in free space:  $Y_{\mathbf{k},s} = k_z/g$  and  $Y_{\mathbf{k},p} = g/k_z$ . The right-hand side (r.h.s.) term  $I_\alpha$  takes into account the overlap between the incident plane wave and the waveguide mode  $|\alpha\rangle$  inside the hole. Considering a normalization for the incident wave such that the energy flux through the hole is unity,  $\text{Re}(\int_{\text{hole}} d\mathbf{S} \mathbf{E}_i \times \mathbf{H}_i^*) = 1$ , we obtain

$$I_\alpha = 2i\sqrt{Y_{\kappa_i}} \langle \kappa_i | \alpha \rangle, \quad (10)$$

where  $Y_{\kappa_i}$  is the admittance of the incident plane wave in free space.

Once the solution of the system of Eqs. (6) is found and the modal amplitudes are known, the normalized-to-area transmission coefficient can be written as

$$T = \sum_{\alpha,\beta} \text{Im}(G_{\alpha\beta}) E'_\alpha E'^*_\beta. \quad (11)$$

Until now we have not mentioned any restrictions on the hole shape, which in our formalism only influences the structure of the waveguide modes  $|\alpha\rangle$ . In this paper, however, we restrict ourselves to the consideration of both circular and rectangular holes, where the waveguide modes are known analytically.

For thick films the solution of Eqs. (6) converges quickly. The reason is that in the subwavelength limit the amplitudes of the waveguide modes decay inside the hole. As the decay is characterized by the propagation constants  $q_\alpha$ , the higher the waveguide mode index, the weaker its influence on the transmission. Therefore, only a few waveguide modes (with the smallest decrements) contribute the transmission.

In contrast, when the thickness  $h$  of the PEC tends to zero, the solution of the system of Eqs. (6) involves many waveguide modes (hundreds or even thousands) to provide the precise result. However, we shall show below that a very accurate computation of the transmission can be performed with some tens of waveguide modes. We shall find the asymptotic value of the transmission by a fitting of the convergent result.

To conclude this section we shall show how to apply the above equations when the bounding dielectric media have permittivities  $\epsilon_I$ ,  $\epsilon_{III}$ . In this case, for a medium with the dielectric constant  $\epsilon$ , the propagation constant of the mode and the admittances become  $k_z = \sqrt{\epsilon g^2 - k^2}$ ,  $Y_{\mathbf{k},s} = k_z/g$  and  $Y_{\mathbf{k},p} = \epsilon g/k_z$ . Then

the wavelength-dependent tensor  $G_{\alpha\beta} = G_{\alpha\beta}(\lambda)$  describing the interaction of the waveguide modes inside the cavity through the EM continuum in vacuum becomes a function of  $\epsilon$ ,  $G_{\alpha\beta}(\lambda; \epsilon)$ . In the upper equation of (6)  $G_{\alpha\beta}$  changes to  $G_{\alpha\beta}(\lambda; \epsilon_I)$ , whereas in the lower to  $G_{\alpha\beta}(\lambda; \epsilon_{III})$ . Working out the expression given by Eq. (9), we find that the relation between the tensors is

$$G_{\alpha\beta}(\lambda; \epsilon) = \sqrt{\epsilon} G_{\alpha\beta}(\lambda/\sqrt{\epsilon}; \epsilon = 1). \quad (12)$$

### III. SMALL HOLE LIMIT

In this section we show how to simplify computation of the transmission when the linear size of the hole,  $a \sim \sqrt{S}$  is small compared to  $\lambda$ . More precisely, we consider the limit

$$\varepsilon \equiv ga \ll 1. \quad (13)$$

In this limit an accurate numerical computation of the tensor  $G_{\alpha\beta}$  becomes problematic. This is related to the orders of magnitude difference between imaginary and real parts of  $G_{\alpha\beta}$ . We have found that in the low-order in parameter  $\varepsilon$  the non-vanishing elements of the tensor depend upon  $\varepsilon$  as (see Appendix A)

$$\text{Im}(G_{\alpha\beta}) \sim \varepsilon^2, \quad \text{Re}(G_{\alpha\beta}) \sim 1/\varepsilon. \quad (14)$$

Both real and imaginary parts of the tensor are important in spite of their substantial difference:  $\text{Re}(G_{\alpha\beta})$  contribute into the amplitude of the waveguide modes (see below), while  $\text{Im}(G_{\alpha\beta})$  takes into account the radiation into free-space [see Eq. (11)]. For  $\varepsilon \ll 1$  the imaginary part of the tensor allows analytical computation, and the real part can be considerably simplified (see details in Appendix A).

In this paper we restrict ourselves to normal-incident wave transmission. In this case the impinging wave can only couple to certain waveguide modes of *TE* type. The analysis of the  $G_{\alpha\beta}$  elements shows that the contribution to the transmission from *TM* waveguide modes is always negligible. This results from both a weak coupling between the waveguide modes of different polarizations inside the small hole, and a weak coupling of *TM* waveguide modes to the EM continuum of vacuum half-spaces.

For the circular hole the incident plane wave couples directly with only the ‘‘horizontal’’  $TE_{1n}$  waveguide modes with integer  $n$  (where the first index indicates the number of semi-periods of the field placed along the polar angle). Coupled between themselves, these waveguide modes are the only ones contributing into the transmission.

For a rectangular hole, when the electric field is directed as shown in Fig. 1, the illuminated waveguide modes are  $TE_{0n}$ , with odd  $n$  (the first and the second

indices define the number of semi-periods of the field placed along  $x$  and  $y$  directions respectively). Only this set of waveguide modes appears in the summation for the transmission according to Eq. (11) [all other elements of  $\text{Im}(G_{\alpha\beta})$  are negligible]. However,  $TE_{0n}$  modes couple to  $TE_{mn}$  ones with even  $m$  and odd  $n$  through the system of Eqs. (6) and must be taken into account.

Due to property expressed in Eq. (14), in the extreme subwavelength limit the transmission coefficient scales as

$$T = \varepsilon^4 \psi(h). \quad (15)$$

The thickness- and shape-dependent function  $\psi(h)$  is given by the solution of the system of Eqs. (6) with appropriately normalized coefficients

$$\psi(h) = \sum_{\alpha,\beta} \tilde{G}_{\alpha\beta} \tilde{E}_\alpha(h) \tilde{E}_\beta^*(h), \quad (16)$$

where

$$\tilde{G}_{\alpha\beta} = \frac{\text{Im}(G_{\alpha\beta})}{\varepsilon^2} \quad \text{and} \quad \tilde{E}_\alpha = \frac{E'_\alpha}{\varepsilon}. \quad (17)$$

The amplitudes  $\tilde{E}_\alpha$  satisfy the system of Eqs. (6), where the imaginary part of the Green tensor is neglected and its real part must be normalized with the small parameter  $\text{Re}(G_{\alpha\beta}) \rightarrow \varepsilon \text{Re}(G_{\alpha\beta})$ . The coefficients of Eq. (8) are replaced by  $G_\alpha^V \rightarrow \varepsilon G_\alpha^V$ ,  $\Sigma_\alpha \rightarrow \varepsilon \Sigma_\alpha$ .

### A. Perfect electric conductor screen

In this subsection we compare the solution based on our formalism with some known results on the transmission through apertures in an infinitesimally thin PEC screen. By reaching an excellent agreement with these results, we justify the applicability of the modal expansion even in the most unfavorable conditions for it.

In the limit  $h \rightarrow 0$ , special care is needed when solving system of Eqs. (6) due to the divergency of the coefficients  $G_\alpha^V$  and  $\Sigma_\alpha$ . In order to remove this divergency, we expand the amplitudes of the waveguide modes over  $gh$

$$\begin{aligned} E_\alpha &= E_\alpha^{(0)} + (gh)E_\alpha^{(1)} + \dots, \\ E'_\alpha &= E_\alpha'^{(0)} + (gh)E_\alpha'^{(1)} + \dots \end{aligned} \quad (18)$$

Equating terms proportional to  $(gh)^{-1}$ , we obtain

$$E_\alpha^{(0)} = -E_\alpha'^{(0)}. \quad (19)$$

Then, keeping terms of zero-order in  $gh$ , we have from Eqs. (6)

$$\begin{aligned} \sum_\beta G_{\alpha\beta} E_\beta^{(0)} - Y_\alpha (E_\alpha^{(1)} + E_\alpha'^{(1)}) &= I_\alpha, \\ \sum_\beta G_{\alpha\beta} E_\beta^{(0)} + Y_\alpha (E_\alpha^{(1)} + E_\alpha'^{(1)}) &= 0. \end{aligned} \quad (20)$$

Adding the two equations in (20) and neglecting the imaginary part of the tensor  $G_{\alpha\beta}$ , due to Eq. (14), we arrive at the final system of equations

$$2 \sum_\beta \text{Re}(G_{\alpha\beta}) E_\beta^{(0)} = I_\alpha. \quad (21)$$

Now, when the film has been converted into a screen with infinitesimal thickness, the amplitudes of the waveguide modes at the incoming and outgoing faces of the film are equivalent. Therefore, the terms  $\Sigma_\alpha$  and  $G_\alpha^V$  responsible for the reflection and coupling of the waveguide modes inside the cavity are not present in Eq. (21), and the waveguide mode amplitudes are coupled by the doubled elements of  $\text{Re}(G_{\alpha\beta})$ .

Using the normalization defined by Eqs. (16), (17), the transmission coefficient can be written in the form (15), where the function  $\psi(h)$  becomes a constant defined by the shape of the hole.

$$T = \varepsilon^4 C. \quad (22)$$

The simplest solution of the system of Eqs. (21) is obtained by retaining only the fundamental waveguide mode. For the circular hole, the Green tensor element corresponding to the fundamental waveguide mode is  $G_{TE_{11}TE_{11}} = 1.1951/\varepsilon + 0.2789i\varepsilon^2$ . For the square hole  $G_{TE_{01}TE_{01}} = 0.9577/\varepsilon + 0.344i\varepsilon^2$ . Within this single-mode approximation, taking the r.h.s. from Appendix A, the transmission pre-factors of Eq. (22) are found immediately: for the circular hole  $C_\circ = 0.1634$  and for the square one  $C_\square = 0.3041$ . For a circular hole, this minimal model provides the transmission of order of 30% with respect to the exact Bethe's result  $C_\circ = 64/(27\pi^2) \simeq 0.2402$ . Therefore, more waveguide modes must be taken into account in order to obtain the correct result.

The convergency of the constant for the circle,  $C_\circ$ , and for the square,  $C_\square$ , with respect to the number of waveguide modes are shown in Fig. 2. After having computed the value of this constant for several tens of waveguide modes, we fit it by a polynomial

$$C = \sum_{m=0}^{m_{\max}} \frac{a_m}{N^m}, \quad (23)$$

where  $N$  is the number of the waveguide modes.

The value  $a_0$  gives us the constant  $C$ . In the calculations shown in Fig. 2, the fitting has been done

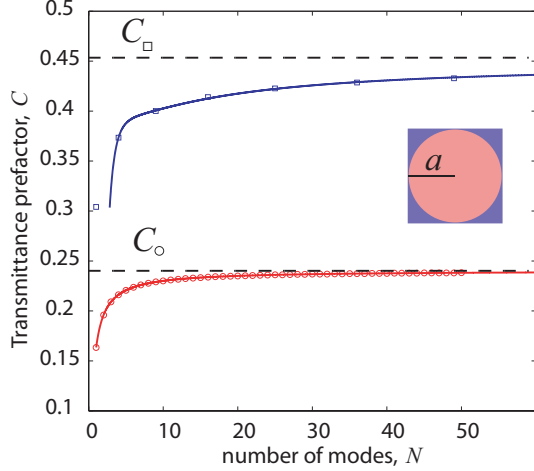


FIG. 2: (Color online) Normalized by  $(ga)^4$  transmittance for the circular and square apertures of the size  $a$  in the PEC screen. The asymptotic values are shown by the dashed lines.

by a forth-order polynomial ( $m_{max} = 4$ ) using 50 waveguide modes. For the circular hole we obtain  $C_○ = a_0 = 0.2403$  with an error of only 0.05% with respect to the exact Bethe's value. For the square hole we obtain  $C_□ \simeq 0.4565$ . Notice that the normalized transmittance through a square hole with the side  $2a$  is about two times larger than that of the round hole with the radius  $a$ .

In the case of rectangular holes, it is useful to write the transmittance as  $T = \varepsilon_x^2 \varepsilon_y^2 C(\tau)$ , where  $\varepsilon_x = a_x g$ ,  $\varepsilon_y = a_y g$  and  $\tau$  is the aspect ratio

$$\tau = a_x/a_y. \quad (24)$$

In this representation  $C(\tau)$  reflects the dependency of the transmittance upon the aspect ratio for a constant area of the hole. As seen from Fig. 3, this dependency is a fast function of  $\tau$ . This is due to a strong dependency of the polarizability of the hole upon the aspect ratio.<sup>17,18</sup> From the point of view of the modal expansion formalism, the cutoff wavelength of the fundamental waveguide mode is  $\lambda_c = 4a_y$ , when the field is parallel to  $x$ -axis. Therefore, the larger the  $a_y$ , the closer the hole to the resonant regime.<sup>14</sup>

We have fitted the dependency shown in Fig. 3 in the region  $\tau \in [1/3, 3]$  by the following function

$$C(\tau) = 0.0132 + 0.2127/\tau + 0.2174/\tau^2. \quad (25)$$

This fitted function provides an excellent approximation to the transmittance: in Fig. 3 the curve given by Eq. (25) is indistinguishable from that obtained from the numeric calculations. In the interval  $\tau < 1$  the dependency  $C(\tau)$  can be extracted from Ref. 18, and we have checked that it coincides with Eq. (25).

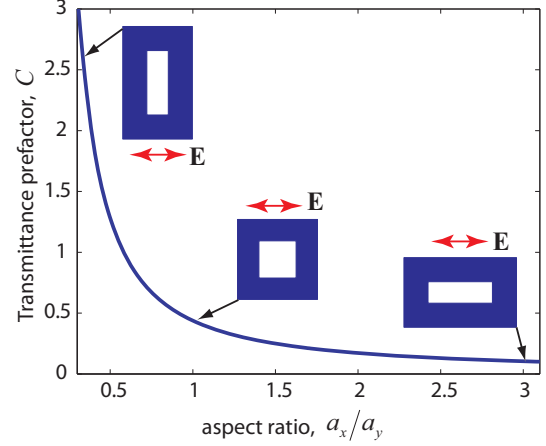


FIG. 3: (Color online) Transmittance for the rectangular aperture in the PEC screen, normalized by  $(ga_x)^2(ga_y)^2$ . The shape of the rectangle for  $a_x/a_y$  equal to 1/3, 1 and 3 is presented.

Let us now turn to the dependency of the transmittance upon dielectric permittivities of the bounding media. Addressing to the general property of  $G_{\alpha\beta}$  in Eq. (12) and to the scaling given by Eq. (14), where  $\varepsilon \sim 1/\lambda$ , we see that the imaginary part of the tensor is a function of  $\epsilon_l$ , namely  $\text{Im}(G_{\alpha\beta}^l) \sim \epsilon_l^{3/2}$ , where  $l = I, III$ . In contrast,  $\text{Re}(G_{\alpha\beta}^l)$  is not dependent upon  $\epsilon_l$ , so that the amplitudes of the waveguide modes depend upon  $\epsilon_I$  only through the r.h.s.,  $E_\alpha, E'_\alpha \sim \sqrt{Y_{\kappa_i}} = \epsilon_I^{1/4}$ . Then it follows directly from Eq. (11) that the transmittance for arbitrary substrate and superstrate is related to the one when the system is in vacuum as

$$T(\lambda, \epsilon_I, \epsilon_{III}) = \sqrt{\epsilon_I \epsilon_{III}^3} T(\lambda, \epsilon_I = 1, \epsilon_{III} = 1) \quad (26)$$

for  $\varepsilon\sqrt{\epsilon_I} \ll 1$ ,  $\varepsilon\sqrt{\epsilon_{III}} \ll 1$ . Note that the transmission is not symmetric with respect to the region of incidence:  $T(\lambda, \epsilon_I, \epsilon_{III}) \neq T(\lambda, \epsilon_{III}, \epsilon_I)$ . This may seem to be paradoxical, as the transmission coefficient of the incident plane wave into the plane wave with the same in-plane wavevector is symmetric due to the symmetry of the scattering matrix. The total transmittance  $T(\lambda)$ , however, takes into account the transmission of a plane wave into a *continuum* of states. As the density of final states depends on the dielectric constant in the transmission region, so does  $T(\lambda)$ . The integration over the scattering amplitudes yields a factor proportional to the wavevector squared modulus in the transmitted medium,  $T \sim (\sqrt{\epsilon_{III}}g)^2 \sim \epsilon_{III}$ , and breaks the  $I$ - $III$  symmetry in Eq. (26).

### B. Thick and medium films

The EM fields inside a subwavelength hole decay exponentially with both the film thickness and the propagation constants of the waveguide modes. In the limit of a very thick film,  $e^{-2|q_{z0}|h} \ll 1$ , the coefficients of Eq. (8) are simplified and the solution of the system of Eqs. (6) can be cast in the matrix form

$$\hat{E} \simeq \hat{D}^{-1} \hat{I}, \quad \hat{E}' \simeq \hat{D}^{-1} \hat{d} \hat{D}^{-1} \hat{I}, \quad (27)$$

where

$$\hat{D} = \|G_{\alpha\beta} + i\delta_{\alpha,\beta} Y_{\alpha}\|, \quad \hat{d} = -2i\|\delta_{\alpha,\beta} Y_{\alpha} e^{iq_{z\alpha}h}\|. \quad (28)$$

Thus, for very thick films the waveguide mode amplitudes on the input side do not depend upon  $h$ , and are of the same order as the incident field. Conversely, the field amplitudes on the output side are exponentially decreased.

For very thick films only the fundamental  $TE$  waveguide mode is expected to contribute into the coupling between both sides of the hole. Therefore, we can retain in the diagonal matrix  $\hat{d}$  only the element corresponding to the fundamental waveguide mode. This means that for a thick film the transmittance decays as  $T \sim e^{-2|q_{z0}|h}$ , where  $q_{z0}$  is the propagating constant of the fundamental waveguide mode. For a rectangular hole with the sides  $2a_x$  and  $2a_y$ ,  $q_{z0} = \sqrt{g^2 - (\pi/2a_y)^2} \simeq i\pi/2a_y$ , and for a circular hole of the radius  $a$ ,  $q_{z0} = \sqrt{g^2 - (u_1/a)^2} \simeq iu_1/a$  (see the definition of  $u_m$  in Appendix A 1). Then for arbitrary film thickness it is useful to rewrite  $T$  given by Eq. (15) in the following form

$$T = \varepsilon^4 e^{-2|q_{z0}|h} C(h), \quad (29)$$

The computations of  $C(h)$  in the interval  $h/a \in [0, 1]$  for both the square and circular holes are shown in Fig. 4. In both cases we phenomenologically adjust this dependency by the function

$$C(h) = C^\infty + (C - C^\infty) e^{-\delta h/a}, \quad (30)$$

containing fitting parameters  $C$ ,  $C^\infty$  and  $\delta$ . In the limit of a screen,  $h = 0$ , Eq. (29) transforms into Eq. (22), while for the infinite film thickness  $f(h)$  becomes a constant  $C^\infty = C(\infty)$ . The constants  $C$  have been given in Subsection III A. The values of the constants for the infinite film thickness have been found to be  $C^\infty_\circ \simeq 0.1694$  and  $C^\infty_\square \simeq 0.3027$ . The values for parameters  $\delta$  are  $\delta_\circ \simeq 6$  and  $\delta_\square \simeq 5$ .

For the rectangle the constants  $C$  and  $C^\infty$  in Eq. (30) are functions of the aspect ratio.  $C = C(\tau)$  is given by Eq. (25), and  $C^\infty = C^\infty(\tau)$  reads

$$C^\infty(\tau) = 0.2298/\tau + 0.08262/\tau^2. \quad (31)$$

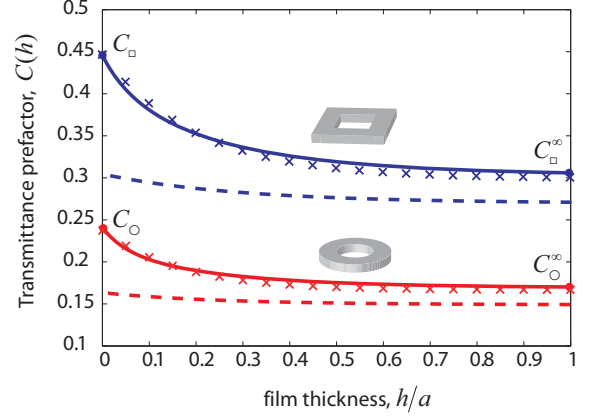


FIG. 4: (Color online) The normalized transmission through small circular and square holes as function of the film thickness. Calculations using only the fundamental waveguide mode are represented by dashed lines. The values for the fitted expression (30) are marked by “x”.

Thus, the formula (29) is applicable for the rectangle as well, if we replace  $\varepsilon \rightarrow \sqrt{\varepsilon_x \varepsilon_y}$  in Eq. (29) and  $h/a \rightarrow h/a_y$  in Eq. (30) (we find that  $\delta$  for the rectangular hole coincides with that for the square hole  $\delta_\square$ ).

In order to make our results more accessible, we summarize in Table I the constants appearing in Eqs. (29) and (30).

As we see from the dependencies shown in Fig. 4, the difference between the full calculation and single-mode approximation decreases when  $h$  increases. For the zero thickness screen it is of order of 30%, and for the limit  $h \rightarrow \infty$  it is of order of 10%. However, if we extract the amplitude of the fundamental waveguide mode from the full (many-mode) solution, and use only this waveguide mode to compute the transmission according to Eq. (11), the difference between this calculation and the exact value is reduced.

TABLE I: Resume of the parameters appearing in the analytical representation of the transmission, see Eqs. (29), (30).

	Circular hole (radius= $a$ )	Square hole (side= $2a$ )	Rectangular hole (sides= $2a_x, 2a_y$ , $\tau = \frac{a_x}{a_y}$ )
$C$	$\frac{64}{27\pi^2}$ (Bethe <sup>1</sup> )	0.4565	$0.0132 + \frac{0.2127}{\tau} + \frac{0.2174}{\tau^2}$
$C^\infty$	0.1694	0.3027	$\frac{0.2298}{\tau} + \frac{0.08262}{\tau^2}$
$ q_{z0} $	$\sqrt{(\frac{u_1}{a})^2 - g^2}$	$\sqrt{(\frac{\pi}{2a})^2 - g^2}$	$\sqrt{(\frac{\pi}{2a_y})^2 - g^2}$
$\delta$	6	5	5

To summarize this section, in the extreme subwavelength regime, many waveguide modes are necessary to provide the precise value for the transmittance. On the

other hand, the fundamental waveguide mode plays a crucial role in the process, especially in the coupling between the fields on top and bottom faces of the hole. As we will show, this reflects the fact that the fundamental waveguide mode possesses the largest induced dipole moment (see Section V below).

#### IV. HOLES OF A MODERATE SIZE

The sizes of apertures used in the experimental samples are often not in the extreme subwavelength limit considered in the previous section. For example, in original experiments on enhanced optical transmission<sup>4</sup> the sizes of the holes were of order of 200 – 300 nm, so the parameter  $\varepsilon$  was  $\varepsilon \gtrsim 1$  in the visible range of the spectra.

In this section we study holes of moderate sizes: still in the subwavelength limit, but with the condition (13) not fulfilled. However, we still consider wavelengths larger than the resonant wavelength of the hole. For the resonant transmission through a single hole at wavelengths close to the cutoff, we refer the reader to Ref. 14.

When the size of the hole increases, the transmittance value can be refined by retaining the next terms in the expansion over  $\varepsilon$ . For a circular aperture in the PEC screen of zero thickness a few first terms were computed by Bouwkamp.<sup>19</sup> However, such a series has radius of convergence  $R_\varepsilon \sim 1$ , and therefore is applicable in a narrow region of  $\varepsilon$ .

For arbitrary film thickness and size of the hole, the transmission can be accurately computed numerically using the modal expansion. But from the practical point of view it is useful to have an analytical formula containing the parameters of the hole. We have numerically computed the transmission through a square hole retaining many waveguide modes in the system of Eqs. (6) in a wide range of the size  $2a$ , and the thickness  $h$ . Then we have approximated the calculations generalizing dependency (29) by adding a quadratic in  $\varepsilon$  term to the function  $C(h)$

$$T = \varepsilon^4 e^{-2|q_{z0}|h} [C(h) + \varepsilon^2 C_2(h)], \quad (32)$$

where  $C_2(h)$  has the same form that  $C(h)$  in Eq. (30)

$$C_2(h) = C_{2\Box}^\infty + (C_2 - C_{2\Box}^\infty) e^{-\delta h/a}. \quad (33)$$

The adjusting constants are  $C_{2\Box}^\infty \simeq 0.66$  and  $C_{2\Box}^\infty \simeq 0.43$ . This dependency provides the transmission with an error not exceeding a few percents in the region  $a/\lambda < 1/6$  (i.e.  $\varepsilon < \pi/3$ ), and for an arbitrary film thickness  $h$ . In the limit of the zero thickness screen, Eq. (32) has a form similar to Bouwkamp's expansion (up to the sixth-order term).<sup>19</sup> However,  $C_2$  is not a constant defining the sixth-order term of the authentic

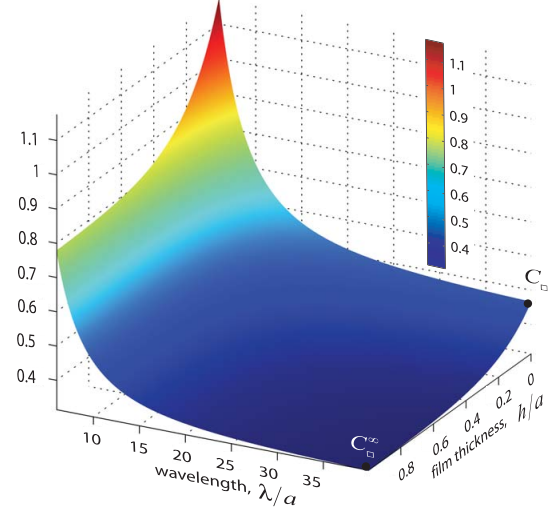


FIG. 5: (Color online) The normalized transmission through small rectangular hole,  $C(h) + \varepsilon^2 C_2(h)$  as a function of the film thickness,  $h/a$  and the wavelength,  $\lambda/a$ , in the units of the hole half-side.

expansion over  $\varepsilon$ . The latter term in the real expansion only refines the value of the transmittance in the small hole limit, meanwhile  $C_2$  results from the fitting of the spectrum captured in a wider region.

#### V. THE HOLE AS A MULTIPOLE

It is well known that the EM field of any source can be considered as resulting from a superposition of multipoles (see e.g. Ref. 2 and references therein). Recently this viewpoint has been used to study the transmission properties of collections of holes.<sup>20</sup> In this section we establish the connection between the mode-matching formalism and the multipole expansion. For this purpose let us focus our attention on the far-field. The in-plane components of the electric field are given by Eqs. (3), and its  $z$ -component can be derived from Maxwell's equations by a straightforward differentiation. The expression for the far-field can be derived with the help of the scalar free-space Green function associated to the Helmholtz equation in three-dimensions.<sup>16</sup> Additionally, in the region of transmission, the expression for the  $\mathbf{E}$  far field, can be computed by using Green's function identities.<sup>3</sup> The expression for  $\mathbf{E}$  in terms of the integration of the field at the face of the hole  $\mathbf{E}_t(\mathbf{r}_t)$  over the hole area is

$$\mathbf{E}_{III}^{far}(\mathbf{r}) = \frac{ig}{2\pi} \frac{e^{igr}}{r} \mathbf{u} \times \int_S dS' \mathbf{n} \times \mathbf{E}'_t(\mathbf{r}'_t) e^{-igr\mathbf{u}\mathbf{r}'}, \quad (34)$$



where  $\mathbf{u}$  is the unit vector pointing into the observation point,  $\mathbf{u} = \mathbf{r}/r$ , and  $\mathbf{n}$  is the external normal. Eq. (34) has the form of retarding potentials<sup>3</sup> resulting from the charges induced by the electric field on the face of the aperture. The field on the face of the hole  $z = h$ , is expressed through the waveguide mode amplitudes

$$\mathbf{E}'_t(\mathbf{r}_t) = - \sum_{\alpha} E'_{\alpha} \langle \mathbf{r}_t | \alpha \rangle. \quad (35)$$

In the reflection region, I, the scattered far-field has a form similar to Eq. (34), but in terms of the field on the interface  $z = 0$ , i.e.,  $-E'_{\alpha}$  is replaced by  $E_{\alpha}$  in Eq. (35).

If we expand the exponent in the integral of Eq. (34),  $e^{-ig\mathbf{u}\mathbf{r}'} = 1 - ig\mathbf{u}\mathbf{r}' + \dots$ , the far-field can then be written in the form of *effective multipoles*<sup>2</sup>

$$\mathbf{E}^{far}(\mathbf{r}) = g^2 \frac{e^{igr}}{r} (\mathbf{u} \times \mathbf{p} + \mathbf{m} + \frac{ig}{2} \mathbf{u} \cdot \hat{\mathbf{Q}}_m + \dots) \times \mathbf{u}, \quad (36)$$

where  $\mathbf{p}$  and  $\mathbf{m}$  are the effective electric and magnetic dipole moments respectively,  $\hat{\mathbf{Q}}_m$  is the effective magnetic quadrupole tensor, etc. Comparing Eq. (36) with Eqs. (34) and (35), we conclude that *each waveguide mode can be interpreted as a superposition of effective multipoles*; the far field then results from the contribution of the multipoles of all the waveguide modes. For example, the effective magnetic and electric dipole moments of the waveguide mode  $|\alpha\rangle$  read

$$\begin{aligned} \mathbf{m}_{\alpha} &= \frac{1}{2\pi ig} \int_S dS' \mathbf{n} \times \langle \mathbf{r}'_t | \alpha \rangle, \\ \mathbf{p}_{\alpha} &= \frac{1}{2\pi} \int_S dS' \mathbf{r}'_t \times [\mathbf{n} \times \langle \mathbf{r}'_t | \alpha \rangle]. \end{aligned} \quad (37)$$

Denoting the dipole moments of the reflection region by  $\mathbf{p}$  and  $\mathbf{m}$ , and those of the transmission region by  $\mathbf{p}'$  and  $\mathbf{m}'$ , we write them as

$$\begin{aligned} \mathbf{m} &= \sum_{\alpha} E_{\alpha} \mathbf{m}_{\alpha}, \quad \mathbf{p} = \sum_{\alpha} E_{\alpha} \mathbf{p}_{\alpha}, \\ \mathbf{m}' &= - \sum_{\alpha} E'_{\alpha} \mathbf{m}_{\alpha}, \quad \mathbf{p}' = - \sum_{\alpha} E'_{\alpha} \mathbf{p}_{\alpha}. \end{aligned} \quad (38)$$

Thus the hole of a finite thickness can be considered as a coupler between induced multipole moments at both faces. For example the systems of Eqs. (38) and (6) describe the coupling between dipole moments that is enough in the low order approximation, when the hole is small. We would like to stress that the effective dipole moments are coupled through all the waveguide modes presented inside the hole. For thick films, however, the contribution of the fundamental waveguide mode dominates over the other modes.

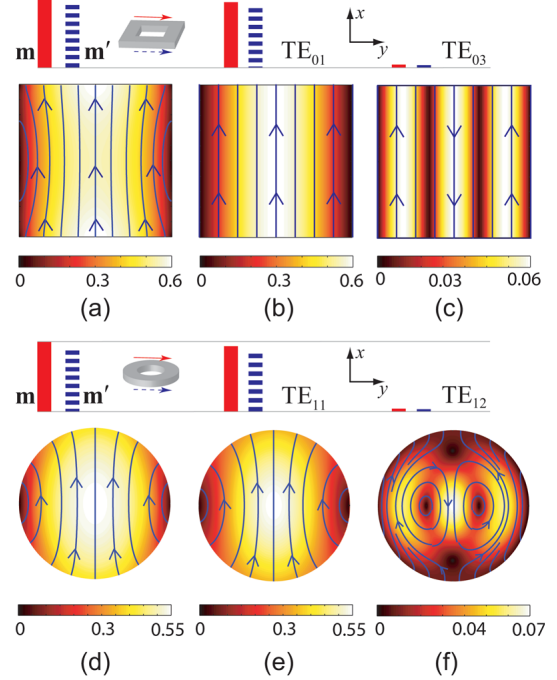


FIG. 6: (Color online) The magnetic dipole moments and the electric field amplitude spatial distribution (at  $z = h/2$ ) for the square and circular holes. The amplitudes of the dipole moments are shown by the bars. The radius of the circular hole is  $a$ , and the side of the square hole is  $2a$ . The considered PEC slab has thickness  $h = 0.1a$ . The distribution of the total electric field modulus together with the electric field lines are shown in (a) and (d). The contribution into magnetic moments from the two lowest waveguide modes and the fields of these waveguide modes are also shown for both hole shapes:  $TE_{01}$  and  $TE_{03}$  of the square are represented in (b) and (c);  $TE_{11}$  and  $TE_{13}$  of the circle are shown in (e) and (f).

Only waveguide modes with zero effective electric dipole moment couple to normal-incident light and generate the far-field. For the circular hole calculations using Eq. (37) show that only “horizontal”  $TE_{1n}$  waveguide modes with integer  $n$  contribute to the magnetic dipole moment. For the rectangular hole the contributing waveguide modes are  $TE_{0m}$  and  $TE_{m0}$  with odd  $m$ . When the incident electric field is directed along  $Ox$  (magnetic field along  $Oy$ ), the magnetic dipole moment induced on the incoming face of the hole with the area  $S$  is<sup>21</sup>

$$\mathbf{m} = \mu S \mathbf{e}_y, \quad \text{where} \quad \mu = \sum_{\alpha} \tilde{E}_{\alpha} C_{\alpha}. \quad (39)$$

We obtain that for the circular and rectangular holes, the constants  $C_{\alpha}$  have the values

$$C_n^{circ} = \frac{1}{i\sqrt{2\pi^3(u_n^2 - 1)}}, \quad C_m^{rect} = \frac{\sqrt{2\tau}}{im\pi^2}, \quad (40)$$



where  $n$  is integer and  $m$  is odd. For the dipole moment  $\mathbf{m}'$  induced on the outgoing face of the film  $\tilde{E}_\alpha$  must be changed to  $-\tilde{E}'_\alpha$ . We have checked that the value for  $\mu$  of the circular hole in the limit of zero-thickness screen (that we obtain with the help of 50 modes),  $\mu_\circ = 0.07624$ , reproduces the Bethe's value  $4/(3\pi^{5/2}) \simeq 0.07622$ . For the square hole we have found  $\mu_\square = 0.08253$ .

Fig. 6 renders the effective dipole moments and the exact fields of the small circular and rectangular hole in the PEC slab of the finite width. The contribution from the fundamental waveguide mode is dominant, so that the field distribution inside the hole is very similar to that of the fundamental waveguide mode. Interestingly, the vector lines of the full field are similar for square and circular holes.

It must be noted that in our method the effective dipoles must be computed after solving the systems of Eqs. (6),(38). We have been unable to derive the equations governing the effective dipoles directly, without previous calculation of the amplitudes  $E_\alpha, E'_\alpha$ .

## VI. CONCLUSIONS

To conclude, this paper has explored the EM transmission through both small and medium-size isolated holes in a perfect electric conductor screen of arbitrary thickness. We have used the modal expansion and have shown that this technique is applicable even in the limit of zero film thickness. This latter limit has been used to check the correctness of the theory through the comparison with Bethe's result. We have phenomenologically fitted the transmittance in a wide region of parameters by simple analytical functions.

We have connected the formalisms based on either modal or multipole expansions, and showed that the induced dipole moments are coupled via all the waveguide modes inside the hole. Our results indicate that the fundamental (lowest-order) waveguide mode possesses the largest dipole moment. It is also responsible for the attenuation of the transmission with the increase of the film thickness,  $T \sim e^{-2|q_{z0}|h}$ .

## VII. ACKNOWLEDGEMENTS

The authors acknowledge support from the Spanish MECD under contract MAT2005-06608-C02 and Consolider Project "Nanolight".

## APPENDIX A: COMPUTATION OF THE GREEN'S TENSOR

Here we give explicit expressions for the tensor  $G_{\alpha\beta}$  in the small hole limit. When the parameter  $\varepsilon$  is small, the integral in Eq. (9) can considerably be simplified. We illustrate these simplifications on the example of the diagonal element for the fundamental mode of the square hole with side  $2a$ . This diagonal element has the following form in polar coordinates ( $q_x = q \cos \theta$ ,  $q_y = q \sin \theta$ ,  $\mathbf{q} = \mathbf{k}/g$ )

$$G_{TE_{01}TE_{01}} = 8i \int_0^{\pi/2} d\theta \int_0^\infty dq \frac{1 - q^2 \sin^2 \theta}{q \sqrt{1 - q^2}} \times \frac{[1 - \cos(2\varepsilon q \cos \theta)][1 + \cos(2\varepsilon q \sin \theta)]}{(4\varepsilon^2 q^2 \sin^2 \theta - \pi^2)^2 \cos^2 \theta}. \quad (\text{A1})$$

We have taken into account the parity of the integrand both in  $q_x$  and  $q_y$ , and, therefore, integrated over the first quadrant of the  $q_x$ - $q_y$  plane only.

We see that the integrand in Eq. (A1) is either purely real or purely imaginary depending only upon the square root  $\sqrt{1 - q^2}$ . Therefore, the integral over  $q$  can be separated into two integrals, one from 0 to 1 (yielding the imaginary part of  $G_{TE_{01}TE_{01}}$ ) and the other from 1 to  $\infty$  (yielding the real part of  $G_{TE_{01}TE_{01}}$ ). Then we expand the integrand for the imaginary part into a series over the parameter  $\varepsilon$ , retain the leading-terms only and take the integral analytically. The result is  $\text{Im}(G_{TE_{01}TE_{01}}) \simeq 32\varepsilon^2/(3\pi^3)$ . To treat the integral for  $\text{Re}(G_{TE_{01}TE_{01}})$ , we make the change of the variable  $\xi = 2q\varepsilon$ . Taking into account that the region  $\xi \lesssim 2\varepsilon$  weakly contribute to the integral, we simplify the square root as  $\sqrt{1 - q^2} \simeq iq$ . Then we replace the lower limit  $\xi = 2\varepsilon$  for  $\xi = 0$  and approximate  $1 - \xi^2 \sin^2 \theta/\varepsilon^2$  by  $-\xi^2 \sin^2 \theta/\varepsilon^2$  in the denominator, so that the real part of  $G_{TE_{01}TE_{01}}$  becomes

$$\text{Re}(G_{TE_{01}TE_{01}}) \simeq -\frac{4}{\varepsilon} \int_0^{\pi/2} d\theta \tan^2 \theta \int_0^\infty d\xi \times \frac{[1 - \cos(\xi \cos \theta)][1 + \cos(\xi \sin \theta)]}{(\xi^2 \sin^2 \theta - \pi^2)^2}. \quad (\text{A2})$$

In order to perform the integration over  $\xi$  analytically, we extend the integrand into the complex plane, changing the trigonometric functions of  $\xi$  to the exponential functions. Finally, Eq. (A2) is derived applying the Residue theorem, by taking into account the presence of the poles on the real axis  $\xi$ . The integral over  $\theta$  is taken numerically.

The other non-vanishing tensor elements both for circular and rectangular holes are simplified analogously. Note, however, that for a circular hole it is

more convenient to perform the analytical integration over  $\theta$  in the real part of  $G_{\alpha\beta}$ , using the identities for the Bessel functions. The integral over  $\xi$  can then be performed numerically.

In the two following subsections we give simplified Green's tensor elements for the rectangular and circular holes.

### 1. Circular hole

Consider a circular hole of radius  $a$ . The imaginary part of the Green tensor is approximated as

$$\text{Im}(G_{TE_{1m}TE_{1m'}}) = \frac{2\varepsilon^2}{3\sqrt{(u_m^2 - 1)(u_{m'}^2 - 1)}}, \quad (\text{A3})$$

where  $u_m$  are the solutions of the equation  $J_1'(u_m) = 0$ . After performing the integration over  $\theta$ , the real part reads

$$\text{Re}(G_{TE_{1m}TE_{1m'}}) = \frac{2}{\varepsilon\sqrt{(u_m^2 - 1)(u_{m'}^2 - 1)}} \times \int_0^\infty d\xi \frac{[\xi J_0(\xi) - J_1(\xi)]^2}{\left[1 - \left(\frac{\xi}{u_m}\right)^2\right] \left[1 - \left(\frac{\xi}{u_{m'}}\right)^2\right]}. \quad (\text{A4})$$

The right-hand side term of Eq. (6) is

$$I_{TE_{1m}} = 2i\sqrt{\frac{2}{u_m^2 - 1}}. \quad (\text{A5})$$

### 2. Rectangular hole

For a rectangular hole with the sides  $2a_x$  and  $2a_y$  the imaginary part of  $G_{\alpha\beta}$  simplifies to

$$\text{Im}(G_{TE_{nm}TE_{n'm'}}) = \delta_{n,0}\delta_{n',0} \frac{32\varepsilon_x\varepsilon_y}{3mm'\pi^3}, \quad (\text{A6})$$

where  $\varepsilon_{x,y} = a_{x,y}g$ . The real part takes the following form

$$\text{Re}(G_{TE_{nm}TE_{n'm'}}) = \frac{1}{\varepsilon_x} \int_0^{\pi/2} d\theta \int_0^\infty d\xi \Phi_{nm;n'm'}(\xi, \theta), \quad (\text{A7})$$

where

$$\Phi_{nm;n'm'}(\xi, \theta) = -\frac{2\sigma_n\sigma_{n'}\sqrt{(n^2 + m^2\tau^2)(n'^2 + m'^2\tau^2)}\xi^4[1 - \cos(\xi\cos\theta)][1 + \cos(\xi\tau^{-1}\sin\theta)]}{\sin^2\theta\cos^2\theta\left[\xi^2 - \left(\frac{n\pi}{\cos\theta}\right)^2\right]\left[\xi^2 - \left(\frac{n'\pi}{\cos\theta}\right)^2\right]\left[\xi^2 - \left(\frac{m\pi\tau}{\sin\theta}\right)^2\right]\left[\xi^2 - \left(\frac{m'\pi\tau}{\sin\theta}\right)^2\right]}. \quad (\text{A8})$$

If  $n = 0$  then  $\sigma_n = \sqrt{2}$  and  $\sigma_n = 2$  otherwise. To simplify the double integral (A7) we transform the cosines in the nominator of  $\Phi$  into exponential functions. The integration over  $\xi$  is performed analytically, extending the integrand into the upper complex half-plane, and using the Residue theorem. The illumination term of

Eq. (6) is

$$I_{TE_{nm}} = \delta_{n,0} \frac{4i\sqrt{2}}{m\pi}. \quad (\text{A9})$$

\* Electronic address: alexeynik@rambler.ru

† Electronic address: lmm@unizar.es

<sup>1</sup> H. A. Bethe, Phys. Rev. **66**, 163 (1944).

<sup>2</sup> J. G. Van Bladel, *Electromagnetic Fields* (Wiley-IEEE, New Jersey, 2007).

<sup>3</sup> J. D. Jackson, *Classical Electrodynamics* (Academic, New York, 1998).

<sup>4</sup> T. W. Ebbesen, H. J. Lezec, H. F. Ghaemi, T. Tio, and P. A. Wolff, Nature **391**, 667 (1998).

<sup>5</sup> A. Roberts, J. Opt. Soc. Am. A **4**, 1970 (1987).

<sup>6</sup> F. J. García de Abajo, Opt. Express **10**, 1475 (2002).

<sup>7</sup> R. Wannemacher, Opt. Commun. **195**, 107 (2001).

<sup>8</sup> E. Popov, N. Bonod, M. Nevier, H. Rigneault, P.-

F. Lenne, and P. Chaumet, Appl. Opt. **44**, 2332 (2005).

<sup>9</sup> S.-H. Chang, S. K. Gray, and G. C. Schatz, Opt. Express **13**, 3150 (2005).

<sup>10</sup> C.-W. Chang, A. K. Sarychev, and V. M. Shalaev, Laser Phys. Lett. **2**, 351 (2005).

<sup>11</sup> A. Degiron, H. J. Lezec, N. Yamamoto, and T. W. Ebbesen, Opt. Commun. B **239**, 61 (2004).

<sup>12</sup> K. J. K. Koerkamp, S. Enoch, F. B. Segerink, N. F. Hulst, and L. Kuipers, Phys. Rev. Lett. **92**, 183901 (2004).

<sup>13</sup> J. W. Lee, M. A. Seo, D. H. Kang, K. S. Khim, S. C. Jeoung, and D. S. Kim, Phys. Rev. Lett. **99**, 137401 (2007).

- <sup>14</sup> F. J. García-Vidal, E. Moreno, J. A. Porto, and L. Martín-Moreno, Phys. Rev. Lett. **95**, 103901 (2005).
- <sup>15</sup> F. J. García-Vidal, L. Martín-Moreno, E. Moreno, L. K. S. Kumar, and R. Gordon, Phys. Rev. B **74**, 153411 (2006).
- <sup>16</sup> J. Bravo-Abad, F. J. García-Vidal, and L. Martín-Moreno, Phys. Rev. Lett. **93**, 227401 (2004).
- <sup>17</sup> S. B. Cohn, Proc. of IEEE **39**, 1416 (1951).
- <sup>18</sup> F. de Meulenaere and J. V. Bladel, IEEE Trans. on Ant. and Prop. **25**, 198 (1977).
- <sup>19</sup> C. J. Bouwkamp, Rep. Prog. Phys. **17**, 35 (1954).
- <sup>20</sup> F. J. García de Abajo, R. Gómez-Medina, and J. J. Sáenz, Phys. Rev. E **72**, 016608 (2005).
- <sup>21</sup> Recall that with our normalization the flux of the incident wave through the hole is unity so that the normalized-to-area transmittance is expressed through  $\mathbf{m}$  as  $T = (4\pi g^4/3)|\mathbf{m}|^2$ .